J Mater Sci (2007) 42:6117–6122
DOI 10.1007/s10853-006-0981-z

Effects of dispersant addition on the synthesis of indium-doped calcium zirconate by co-precipitation techniques

Vivek Krishnan · Jeffrey W. Fergus

Received: 3 May 2006 / Accepted: 19 September 2006 / Published online: 16 April 2007

Abstract The synthesis of In_2O_3-doped $CaZrO_3$ by solid oxide and oxalate co-precipitation routes has been studied. The effects of using polymeric surfactants (PEG) and ball milling on the synthesis were determined by characterizing the materials at various stages using SEM, XRD, FTIR and particle size analysis. PEG addition and ball milling led to the formation of smaller particles which reduces the time and temperature needed for perovskite formation.

Introduction

Perovskites of the type ABO_3 display a wide range of chemical compositions and attributes, and for this reason have been called ''inorganic chameleons'' [1]. Calcium zirconate ($CaZrO_3$) forms the perovskite structure and possesses excellent mechanical, optical and electrical properties. Stoichiometric $CaZrO_3$ maintains low electronic conductivity at very low oxygen partial pressures and has been considered as a replacement for stabilized zirconia in oxygen probes for steel melts [2]. Trivalent-doped $CaZrO_3$ (e.g. In^{3+},Y^{3+},Yb^{3+}) conducts protons in humid or hydrogen-containing atmospheres [3–5] which, along with its excellent chemical and mechanical stability, makes it a prime candidate for hydrogen sensing applications in liquid aluminum and copper [6–8]. $CaZrO_3$ based materials also have a high dielectric constant (~30) and a low loss tangent (quality factor of 3000 at 13 GHz) leading to their being investigated as a potential material for CMOS applications [9, 10].

V. Krishnan (✉) · Jeffrey W. Fergus
Materials Research and Education Center, Auburn University, Auburn, AL, USA
e-mail: vkrishnan@mmm.com

The properties of $CaZrO_3$ depend on the synthesis method employed. The most common method for powder synthesis is the solid mixing technique using $CaCO_3$ and ZrO_2 as starting materials [11, 12]. Although the method is simple and inexpensive, wet chemical methods like sol–gel [13, 14], hydrothermal routes and co-precipitation can improve cation homogeneity and reduce the temperatures required for phase formation [15, 16]. These methods also help produce more surface active powders that sinter better and thus produce higher density ceramics [17].

Among the various wet chemical techniques used for the synthesis of doped and undoped $CaZrO_3$, oxalate co-precipitation has received wide attention [18–20]. The technique involves precipitation of metal oxalate precursors from the reaction between a cationic solution and a chelating agent (e.g. oxalic acid). These powders thermally decompose to produce the desired perovskite phase. Agglomeration, which is detrimental to sintering, can occur in the solution phase, so ionic and non-ionic polymeric surfactants that use electrostatic or steric effects to reduce particle size have been used [21].

This paper examines a co-precipitation technique for the synthesis of In_2O_3-doped $CaZrO_3$. Perovskite formation from the decomposition of oxalate precursors is compared to that for the solid oxide route of synthesis. The effects of adding polyethylene glycol (PEG-$HO(CH_2CH_2O)_nH$) as a dispersant and reducing particle size by mechanical means are also discussed.

Experimental

The perovskite $CaZr_{0.9}In_{0.1}O_{2.95}$ was synthesized using solid oxide and co-precipitation methods. In the solid oxide method, stoichiometric amounts of $CaCO_3$ (99.5%), ZrO_2

(99.9%), In_2O_3 (99.99%) were crushed together using a mortar and pestle and ball milled for 5 days in ethanol with a 3:1 ratio of ethanol to powder. $CaCO_3$ was used instead of CaO as this has been reported to produce a more active calcium species [22]. The solid mixture was then calcined in air at various times and temperatures using a tube furnace or a muffle furnace.

For the synthesis using co-precipitation, calculated amounts of $ZrOCl_2 \cdot 8H_2O$ (99.9%), $CaCO_3$ and In_2O_3 were dissolved in a 1:1 solution of HCl and distilled water at 70 °C with constant stirring. The acidic solution containing a mixture of the ions (Ca^{2+}, Zr^{4+}, In^{3+}) was then added dropwise into an alkaline solution of oxalic acid, which was maintained at pH 9 by adding NH_4OH. The resultant solution was stirred continuously for 30 min and then aged for 3 h. The aged solution was filtered and the precipitate was washed three times using water to remove Cl^- ions. An $AgNO_3$ solution was used to check for any residual Cl^- contaminants, as a curdy white precipitate of AgCl would form immediately if Cl^- was present. A final washing step was carried out using an ethanol solution. The precursor powder was dried for 12 h at 70 °C and then calcined for perovskite formation.

To investigate the effect of dispersant addition, 5 wt.% PEG 200 was added to the cationic solution before addition into the oxalate solution. An equal quantity of a higher molecular weight polymer PEG 1450 was added after the salt solution was added to the oxalic acid. The remaining steps of the synthesis process were not changed. For the investigation of ball milling effects, a batch of precursor powders was prepared without any dopant. The powders were ball milled with ethanol in a ratio 1:3 by weight for 2 days. The slurry was then dried and calcined for desired phase formation.

All powders were characterized using scanning electron microscopy (SEM), X-ray diffraction (XRD) and electron dispersive X-ray spectroscopy (EDS). Particle size analysis was accomplished using laser scattering. Fourier transform infra-red spectroscopy (FTIR) measurements were made in the transmissive mode using pellet samples fabricated by uniaxial pressing of the powders with KBr.

Results and discussion

Comparison of synthesis techniques

$CaZrO_3$ forms the orthorhombic perovskite structure (a = 0.55912 nm, b = 0.80171 nm, c = 0.57616 nm) [23] at temperatures up to 1750–2000 °C, above which a cubic phase has been reported [24, 25]. The XRD spectra in Fig. 1 confirm the formation of the perovskite phase in powders prepared from the solid oxide route. A secondary

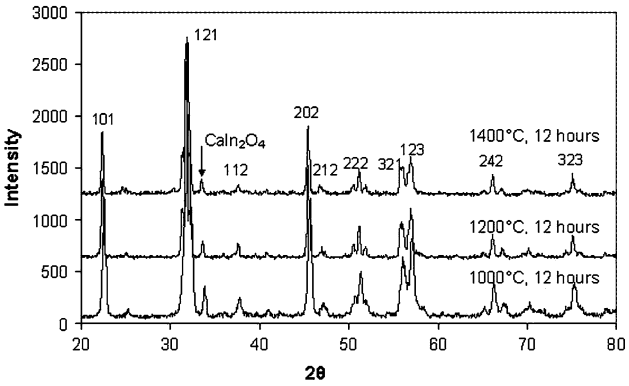

Fig. 1 $CaZr_{0.9}In_{0.1}O_{2.95}$ prepared from calcination of solid oxides for 12 h at various temperatures. Peaks indexed according to JCPDS card 35-0790

peak (2θ = 32.9°) corresponding to the In-rich $CaIn_2O_4$ phase is also present which suggests that the indium did not completely dissolve in the perovskite lattice.

Figure 2 shows XRD results from oxalate precursor powders prepared using the co-precipitation technique. All the crystalline peaks shown can be attributed to the $CaC_2O_4 \cdot H_2O$ phase based on the JCPDS reference card. While the presence of this phase is consistent with other published reports, there is some disagreement over the other phases present in the system [26–28]. For example, Wei et al. and Le et al. report the presence of a $ZrC_2O_4 \cdot H_2O$ phase in the precursor material based on XRD data. However, the XRD peaks attributed to this phase are either very small or match closely with those of $CaC_2O_4 \cdot H_2O$. Following the work of Le et al., van Rij et al. conducted a more thorough investigation of this system and concluded that $CaC_2O_4 \cdot H_2O$ was the only major crystalline phase present in the precursor powder.

The precipitation of zirconium in the form of hydrous oxides has been discussed previously by Baes and Mesmer [29]. Other researchers have explained the presence of these phases in the form of amorphous humps in the XRD

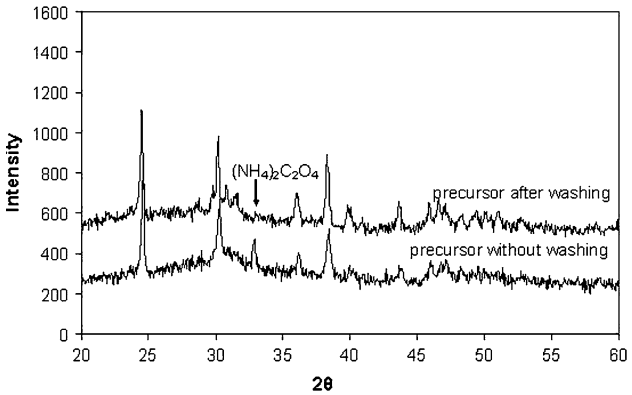

Fig. 2 Precursors formed by the oxalate co-precipitation process

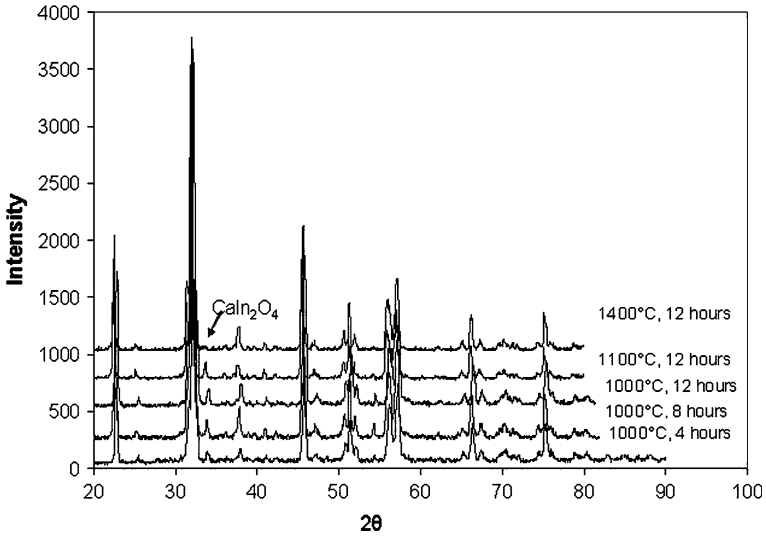

Fig. 3 $CaZr_{0.9}In_{0.1}O_{2.95}$ prepared from oxalate precursors decomposed at different temperatures and times

spectra [30]. The XRD spectra in Fig. 2 contain broad peaks at ~30° suggesting that zirconium is present in an amorphous phase. Although XRD peaks for an In-rich phase were not present, EDX results confirmed presence of the dopant in the desired proportions. Figure 2 contains an additional XRD peak in the spectrum for powders prepared without using the elaborate washing procedure. The peak can be attributed to ammonium oxalate, the presence of which was further confirmed with FTIR results that showed a characteristic peak at 2950 cm^{-1}. Ammonium oxalate has been found to inhibit sintering in other oxide systems [31], so careful washing of the powder is an important step in the precursor powder preparation.

The oxalate precursor powders decompose to form the perovskite at temperatures higher than 850 °C. The XRD data in Fig. 3 shows disappearance of the $CaIn_2O_4$ peaks when the sample is calcined at 1400 °C. The decreasing amount of $CaIn_2O_4$ with thermal treatment is represented in Fig. 4 by the ratio of integrated peak intensities of $CaIn_2O_4$ (32.9°) and (121) $CaZrO_3$ (22.35°). The $CaIn_2O_4$ peaks decrease more rapidly in samples calcined at 1400 °C as compared to samples calcined at 1200 °C, presumably due to faster diffusion at the higher temperature.

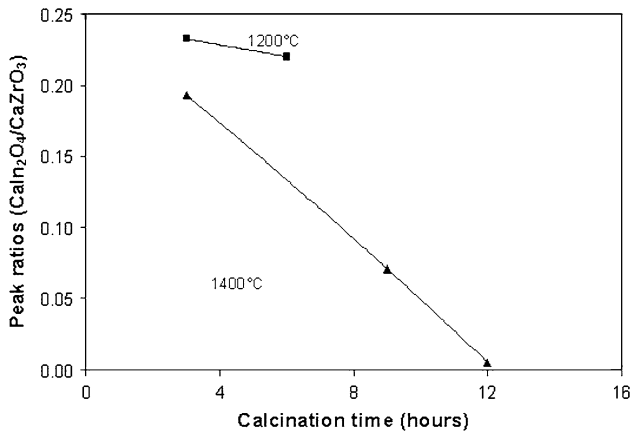

Fig. 4 Decrease in $CaIn_2O_4$ peak with increasing calcination times

Effect of dispersant addition

PEG could lead to reduced particle size either by inhibiting agglomeration or by causing redispersion of agglomerated particles formed earlier in the process. Mechanisms based on both of these effects have been proposed in the literature.

The first mechanism explains particle size reduction based on PEG's ability to prevent agglomeration. Since PEG is a non-ionic polymer, it consists of neutral hydrophobic and hydrophilic parts. The O–H bonds are, however, polar and should form linkages within the system by hydrogen bonding. According to Liu et al. [32] and Ece et al. [33], the interfacial energy at the particle/liquid interface is reduced because of these surface linkages as the adsorbed polymer produces repulsive forces between the suspended particles. Steric stabilization of the dispersion results in limited particle–particle interactions and reduced agglomeration. A schematic of particles separated by PEG molecules is shown in Fig. 5.

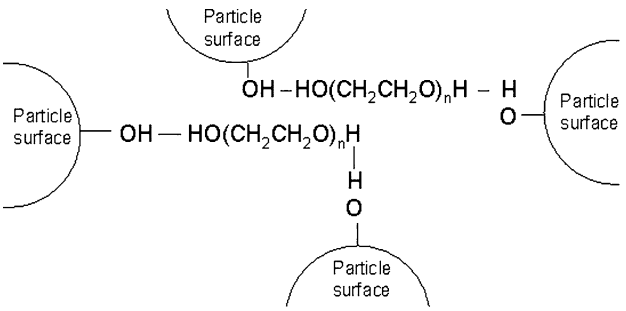

Fig. 5 Surface PEG layers adsorbed on precursor particle

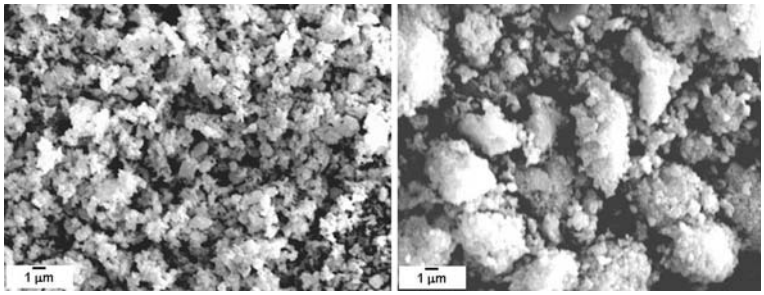

Fig. 6 SEM image of powders prepared with and without PEG (3500×)

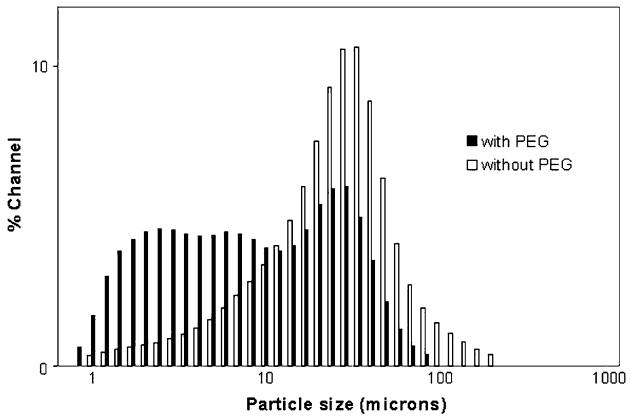

Fig. 7 Effect of surfactant PEG on size distribution of oxalate precursor powders

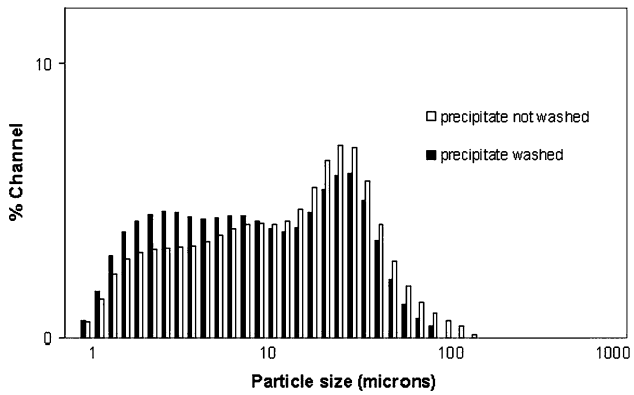

Fig. 8 Effect of powder washing on size distribution of oxalate precursor powders

Uhland et al. [34] propose a different mechanism in which PEG is said to promote deagglomeration and redispersion of particles. According to this model, osmotic pressure is created due to a change in the chemical potential of the solvent within and outside the agglomerate. Since the osmotic pressure is inversely related to the molecular weight of the polymer, (vant Hoff's law), a lower molecular weight PEG should be more effective in breaking down larger agglomerates. SEM micrographs of Fe–Ni double oxalates shown by Uekawa et al. [35] confirm particle size increases with increasing molecular weight of PEG.

SEM investigation of the powders synthesized in this work (Fig. 6) shows that PEG reduces particle agglomeration. The particles produced with PEG are smaller and less agglomerated than those produced in the absence of PEG. The particle size distribution in Fig. 7 shows that the powders synthesized without PEG consist mainly of larger particles with a relatively narrow distribution. The addition of PEG results in a wider distribution with an increase in the amount of smaller agglomerates.

Washing of the precursor powders with ethanol and water affects the particle size distribution as shown in Fig. 8. Although the distribution does not change as much as for PEG addition, smaller particles are formed with washing. According to Kaliszewski and Heuer [36], the ethanol treatment aids in the formation of surface ethoxide groups, which inhibits growth of inter-particle bridges by displacing adsorbed water that causes hydrogen bonding between the polar water molecules.

The PEG addition improves the kinetics of perovskite formation as shown in the XRD of precursors decomposed at 850 °C (Fig. 9). XRD spectra of powders prepared without PEG contain a large peak matching with the

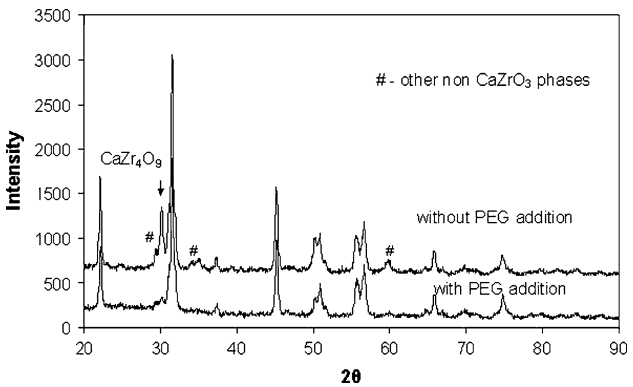

Fig. 9 Influence of PEG on formation of $CaZrO_3$ from oxalate co-precipitation process

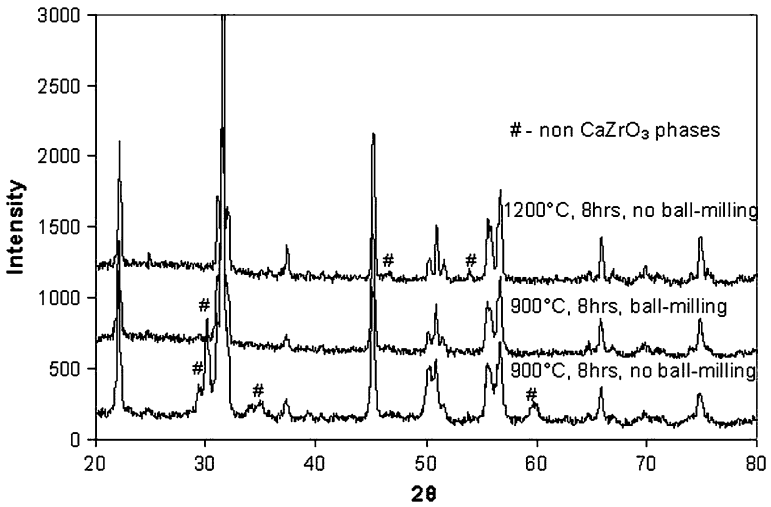

Fig. 10 Effect of precursor ball milling on formation of $CaZrO_3$ from oxalate co-precipitation

Zr-rich φ_1 phase ($CaZr_4O_9$) and several other unidentified peaks (marked with #), while powders prepared with PEG contain only peaks from $CaZrO_3$.

Particle size reduction by mechanical means also brings about similar results in this oxide system. The XRD results in Fig. 10 show that powders milled for 2 days prior to decomposition form the perovskite after calcinations at 900 °C while powders that were not milled contain additional phases after the same heat treatment. Some additional peaks are still present in the unmilled powders even after calcining at a higher temperature of 1200 °C.

Conclusions

The oxalate co-precipitation process has been used to synthesize In_2O_3 doped $CaZrO_3$ at lower times and temperatures as compared to the solid oxide method. The reduction in agglomerate size by chemical methods (addition of PEG) and mechanical means (ball milling) improves the kinetics of the synthesis process.

Acknowledgements The authors wish to acknowledge funding received from the NASA-sponsored Solidification Design Consortium directed by Dr. Tony Overfelt, Auburn University. We thank Achmad Hanafi for his contribution to the development of the precipitation process and graduate students Rui Shao and George Teoderescu for their help with particle size and FTIR measurements.

References

1. Islam MS (2000) J Mater Chem 10:1027
2. Janke D (1982) Metall Trans B 13B:227
3. Iwahara H, Yajima T, Hibino T (1993) Solid State Ionics 61:65
4. Kurita N, Fukatsu N, Ito K, Ohashi T (1995) J Electrochem Soc 142:1552
5. Kobayashi K, Yamaguchi S, Iguchi Y (1998) Solid State Ionics 108:355
6. Park D, Hwang J (2005) US Pat Appl Publ
7. Krishnan V, Fergus JW, Fasoyinu F In: ASM International, Materials Park (ed) Proceedings of the 2nd international aluminum casting technology symposium, Columbus, OH, October 2002, p 155
8. Kurita N, Fukatsu N, Miyamoto S, Sato F, Nakai H, Irie K, Ohashi T (1996) Metall Mater Trans B 27B:929
9. Yu T, Chen CH, Chen XF, Zhu W, Krishnan RG (2004) Ceram Int 30:1279
10. Zhu W, Yu T, Chen CH, Chen XF, Krishnan RG (2004) Integrated Ferroelectrics 61:25
11. Angers R, Tremblay R, Chaklader ACD (1972) J Am Ceram Soc 55:425
12. Angers R, Tremblay R, Chaklader ACD (1974) J Am Ceram Soc 57:231
13. Yu T, Zhu WG, Chen CH, Chen XF, Gopal Krishnan R (2004) Physica B 348:440
14. Xu J, Wilkinson A, Pattanaik S (2000) Chem Mater 12:3321
15. Gonenli E, Tas C (1999) J Eur Ceram Soc 19:2563
16. Saavedra MJ, Parada C, Figueiredo MO, Correa Dos Santos A (1993) Solid State Ionics 63–65:213
17. Laberty-Robert C, Ansart F, Castillo S, Richard G (2002) Solid State Sci 4:1053
18. Zheng W (1994) Chemical Research in Chinese Universities, vol. 10, p 333
19. Gangadevi T, Muraleedharan K, Kannan MP (1989) Thermo Acta 146:225
20. Reddy VB, Mehrotra PN (1981) J Inorg Nucl Chem 43:1078
21. Jean J-H, Wang H-R (1998) J Am Ceram Soc 81:1589
22. Nadler MR, Fitzsimmons ES (1955) J Am Ceram Soc 38:214
23. Koopmans HJA, Van De Velde GMH, Gellings PJ (1983) Acta Cryst C39:1323
24. Joint Council of Powder Diffraction Standards (JCPDS) card 35-0790 (2001)
25. Figs Zr-061 and Zr-065 (1998) Phase diagrams for zirconium and zirconia systems. In: Ondik HM, McMurdie HF (eds) American Ceramics Society, Westerville, OH
26. Wei Y, Guangqiang L, Zhitong S (1998) J Mater Sci Lett 17:241
27. Le J, Van Rij N, Van Landschoot RC, Schoonman J (1999) J Eur Ceram Soc 19:2589
28. Van Rij N, Winnubst L, Le J, Schoonman J (2000) J Mater Chem 10:2515

29. Baes CF Jr, Mesmer RE (1976) The hydrolysis of cations. John Wiley and Sons p 152
30. Vasylkiv O, Sakka Y, Borodians'ka HJ (2001) J Am Ceram Soc 84:2884
31. Cavalheiro A, Zaghete MA, Varela J (1999) Cerâmica 45:56
32. Liu Q, Gao L, Yan D, Mandal H, Thompson DP (1997) J Eur Ceram Soc 17:581
33. Ece OI, Alemdar A, Gungor N, Hayashi S (2002) J Appl Polym Sci 86:341
34. Uhland SA, Cima MJ, Sachs EM (2003) J Am Ceram Soc 86:1487
35. Uekawa N, Ichikawa H, Itsuki A, Ishii S, Kakegawa K, Sasaki Y (2000) Chemical Society of Japan 3:187
36. Kaliszewski MS, Heuer AH (1990) J Am Ceram Soc 73:1504